AGU PUBLICATIONS

Geophysical Research Letters

RESEARCH LETTER
10.1002/2015GL066389

Key Points:
- OIB QL snow depth on sea ice retrieval performs well in level ice environments
- Deformed first-year and multiyear ice are difficult retrieval environments for the OIB QL product
- Surface roughness contributes to diminished correlation between measured and retrieved snow depths

Supporting Information:
- Supporting Information S1

Correspondence to:
J. King,
joshua.king@ec.gc.ca

Citation:
King, J., S. Howell, C. Derksen, N. Rutter, P. Toose, J. F. Beckers, C. Haas, N. Kurtz, and J. Richter-Menge (2015), Evaluation of Operation IceBridge quick-look snow depth estimates on sea ice, *Geophys. Res. Lett.*, *42*, 9302–9310, doi:10.1002/2015GL066389.

Received 2 OCT 2015
Accepted 10 OCT 2015
Accepted article online 14 OCT 2015
Published online 6 NOV 2015

Evaluation of Operation IceBridge quick-look snow depth estimates on sea ice

Joshua King[1], Stephen Howell[1], Chris Derksen[1], Nick Rutter[2], Peter Toose[1], Justin F. Beckers[3], Christian Haas[3,4], Nathan Kurtz[5], and Jacqueline Richter-Menge[6]

[1]Climate Research Division, Environment Canada, Toronto, Ontario, Canada, [2]Department of Geography, Northumbria University, Newcastle upon Tyne, UK, [3]Department of Earth and Atmospheric Sciences, University of Alberta, Edmonton, Alberta, Canada, [4]Department of Earth and Space Science & Engineering, York University, Toronto, Ontario, Canada, [5]Hydrospheric and Biospheric Sciences Laboratory, NASA Goddard Space Flight Center, Greenbelt, Maryland, USA, [6]Cold Regions Research and Engineering Laboratory, Engineer Research and Development Center, Hanover, New Hampshire, USA

Abstract We evaluate Operation IceBridge (OIB) "quick-look" snow depth on sea ice retrievals using in situ measurements taken over immobile first-year ice (FYI) and multiyear ice (MYI) during March of 2014. Good agreement was found over undeformed FYI (−4.5 cm mean bias) with reduced agreement over deformed FYI (−6.6 cm mean bias). Over MYI, the mean bias was −5.7 cm, but 54% of retrievals were discarded by the OIB retrieval process as compared to only 10% over FYI. Footprint scale analysis revealed a root-mean-square error (RMSE) of 6.2 cm over undeformed FYI with RMSE of 10.5 cm and 17.5 cm in the more complex deformed FYI and MYI environments. Correlation analysis was used to demonstrate contrasting retrieval uncertainty associated with spatial aggregation and ice surface roughness.

1. Introduction

Knowledge of snow on sea ice is important because its large air content makes it an effective insulator which influences winter ice growth [e.g., *Perovich et al.,* 2003] and its high albedo reduces the amount of solar radiation absorbed into sea ice influencing melt processes during summer [e.g., *Perovich et al.,* 2007]. Snow depth is also a requirement for altimetry-based retrieval of sea ice properties (e.g., ice thickness), whereby inadequate knowledge of snow depth distribution directly impacts the availability and quality of derived products [*Giles et al.,* 2007; *Kern et al.,* 2015; *Ricker et al.*, 2015]. Despite its broad importance, remotely sensed estimates of snow depth on sea ice have previously only been available from coarse resolution passive microwave data [e.g. *Comiso et al.,* 2003; *Brucker and Markus*, 2013; *Maass et al.,* 2015]. However, in 2009 as a result of the introduction of NASA's Operation IceBridge (OIB), high-resolution airborne estimates of snow depth on sea ice over both, seasonal first-year ice (FYI) and multiyear ice (MYI) in the western Arctic, have become available during the months of March and April [*Koenig et al.,* 2010; *Kurtz et al.,* 2013]. This expansive data set has been used to characterize Arctic distributions of snow on sea ice [*Kurtz and Farrell,* 2011; *Webster et al.,* 2014], validate satellite retrieval products [*Brucker and Markus,* 2013; *Maass et al.*, 2015; *Armitage and Ridout,* 2015] and initialize sea ice forecasting models [*Lindsay et al.,* 2012].

Public release of OIB products has typically required more than 1 year between data collection and distribution. In order to accommodate time-sensitive applications (e.g., initialization of seasonal forecast models), an expedited "quick-look" (QL) product was introduced in 2012 providing 40 m along-track estimates of snow and sea ice properties within 1 month of collection. OIB estimates of snow depth on sea ice rely on automated identification of the air-snow and snow-ice interfaces in the response of the University of Kansas ultrawideband snow radar [*Panzer et al.,* 2013] to translate propagation delay into layer thickness [see *Kurtz et al.,* 2013]. This retrieval process is known to include geophysical uncertainty (e.g., surface roughness) [*Farrell et al.*, 2012; *Newman et al.*, 2014], as well as system-based uncertainty related to the presence of coherent noise, predominate radar side lobes, and the finite-range resolution of the snow radar [*Kwok and Maksym*, 2014; *Newman et al.,* 2014; *Holt et al.*, 2015; *Kwok and Haas*, 2015]. To accelerate release, the QL product uses field-processed snow radar returns that may be subject to system-based uncertainty unaccounted for in the postprocessed archival error estimate of 5.7 cm [*Kurtz et al.,* 2013; *Webster et al.,* 2014].

At the time of this study, the QL product represents the only estimates of snow depth on sea ice available to potential users of data from the OIB Arctic 2014 campaign. While previous evaluation of the QL product has demonstrated reasonable accuracy over level FYI and general agreement with the archival product [*Webster et al.,* 2014], validation to date is based on a limited number of field data sets. Given the recent identification of campaign specific variations in the snow radar signal [*Kwok and Haas*, 2015], as well as the significant influence of local ice surface topography [*Newman et al.,* 2014], there is an immediate need to evaluate uncertainty in the current QL product to align community expectations and provide guidance for its use. To do so, we assess a subset of the 2014 QL estimates of snow depth on sea ice using spatially extensive in situ measurements collected along the flight tracks of two OIB missions.

2. Data and Methods

Uncertainty of the QL snow depth on sea ice estimates was evaluated with coincident in situ measurements taken over regions of FYI near Eureka, Nunavut in the Canadian Arctic Archipelago, and over MYI in the Lincoln Sea approximately 50 km off the coast of northern Greenland (Figure 1a). In each case, flights were completed over immobile sea ice, requiring no geolocation correction prior to evaluation. For the FYI site, a dedicated OIB mission took place on 25 March 2014 where a predetermined set of 11 parallel flight lines, ~50 km in length, were flown within Eureka Sound (Figure 1b). Flight lines were spaced 12 m apart to maximize the potential for coincidence between planned in situ measurements and the narrow footprint of the OIB snow radar (10 m across-track from *Panzer et al.* [2013]). In total, 13,604 QL retrievals were generated over the combined 550 km transit of the OIB aircraft. On 31 March 2014, an additional 11 flight lines were completed without intentional offset over immobile MYI in the Lincoln Sea (Figure 1c). Each repeat pass of the MYI site was ~1.3 km in length, resulting in a total of 337 retrievals. The QL estimates of snow depth on sea ice associated with each mission were made available for download from the National Snow and Ice Data Centre on 12 May 2014 (http://nsidc.org/data/docs/daac/icebridge/evaluation_products/sea-ice-freeboard-snowdepth-thickness-quicklook-index.html).

To characterize coincident variations in snow depth, linear sampling transects were established under both sets of OIB flight lines. Timely delivery (within ~12 h) of the aircraft position data allowed surface measurements to be completed with strong spatial coincidence and in rapid succession of each airborne mission. Measurements of snow depth were made with multiple Global Positioning System (GPS) enabled Snow-Hydro Magnaprobes (http://www.snowhydro.com) which have an expected depth precision of 3 mm [*Sturm et al.,* 2006]. Between 26 March 2014 and 3 April 2014, 37,320 colocated measurements were acquired over a distance of ~46 km at the FYI site (~2 m spacing; Figure 1b). In addition to measurements completed parallel to the OIB flight direction (along-track), orthogonal transects of up to 100 m were sampled at random intervals to evaluate variation in the radar range direction (across-track). Measurements at the MYI site were completed using a larger horizontal spacing of ~5 m to accommodate transit of the more complex ice topography. In total, 250 depths were collected over the 1.3 km unidirectional MYI transect [*Beckers et al.*, 2015].

As a first step in evaluating the QL retrievals, an effort was made to equate differences in the length scale characterization of the surface and airborne measurements (i.e., an effective submeter footprint in situ versus the 40 m QL product). Individual in situ measurements were spatially averaged to create a 40 m along-track mean using the southernmost measurement as a point of origin. To ensure meaningful colocation between the in situ and airborne data sets, a maximum distance for comparison was identified based on observed length scales of variability. Variograms were used to quantify the distance over which in situ measurements were likely to be unrelated (see *Iacozza and Barber* [1999] and *Sturm et al.* [2002] for extended discussion). An assumption was made that in situ and airborne measurements separated at distances greater than the identified length scales would also be uncorrelated and were removed prior to evaluation against statistical summaries of the in situ transects.

To extend evaluation of the colocated measurements, an approximation of the QL footprint was created by estimating the dimensions of the pulse-limited snow radar case. Assuming a smooth ice surface, the radius of the pulse-limited footprint was estimated using $r_{pl} = \sqrt{ch/B}$, where c is the speed of light, h is altitude above the surface, and B is the radar bandwidth [*Panzer et al.,* 2013]. Altitude above the ice surface, h, was calculated as the mean difference of a minimum of 200 flight and ice surface elevations closest to each QL centroid. Flight elevations and ice surface heights were extracted from the Position/Avionics L1B [*Dominguez,* 2010]

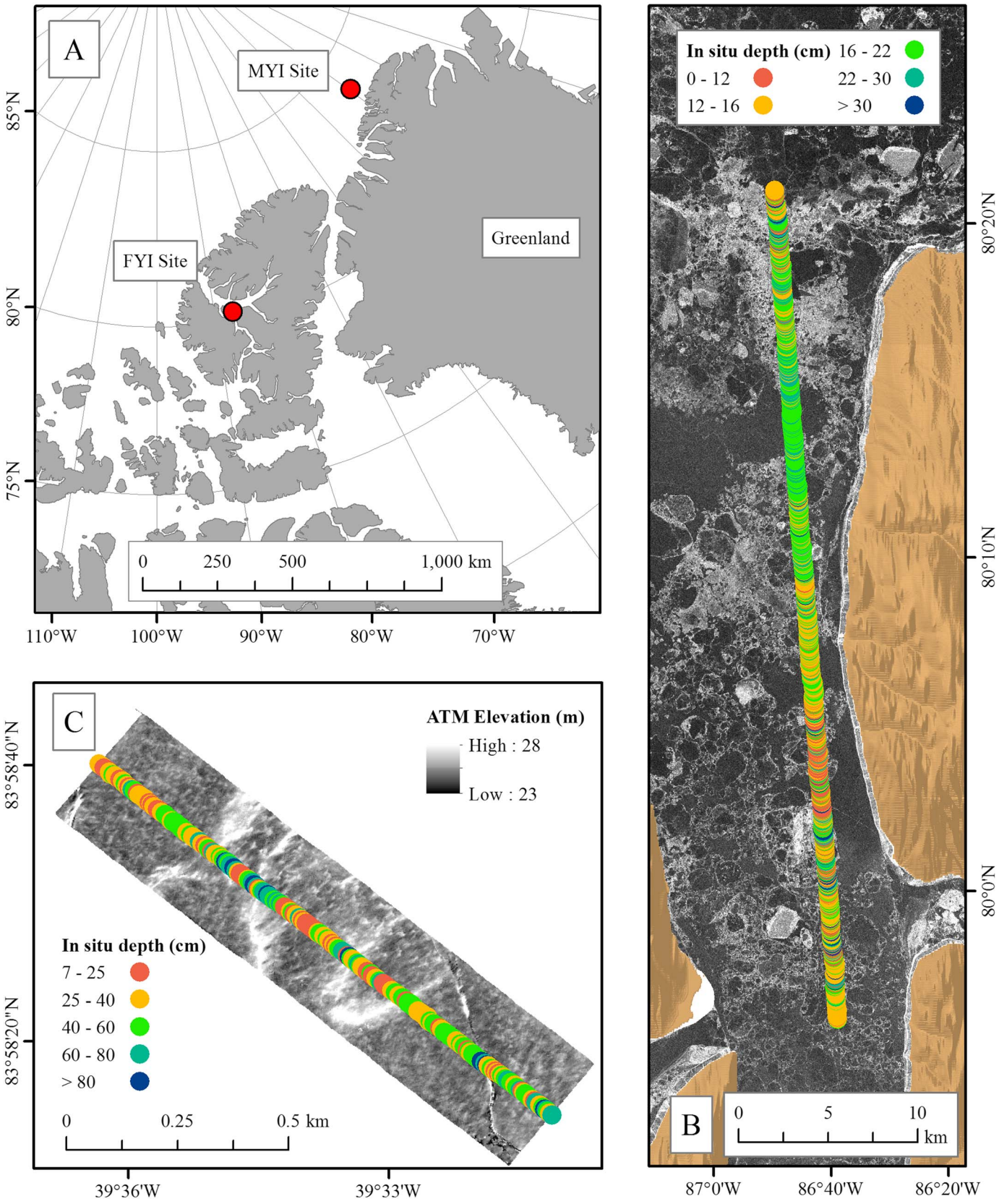

Figure 1. (a) Study locations and in situ transects for the (b) FYI and (c) MYI sites. The background of Figure 1b shows RADARSAT-2 backscatter (RADARSAT imagery © Canadian Space Agency) collected 24 March 2014.

and Airborne Topographic Mapper (ATM) L1B [*Krabill,* 2013] data sets, respectively. The along-track dimension and orientation of each footprint were defined by the 40 m resolution of the QL product and the direction between successive QL centroids. Colocated in situ measurements were extracted within each footprint to derive summary statistics. Those with less than 10 extracted measurements were discarded to limit the influence of outliers in undersampled footprints. Due to the limited number of measurements available at the MYI site, a smaller threshold of five was necessary.

3. Results and Discussion

3.1. Assessment of In Situ Measurements and QL Retrievals Along Transects

3.1.1. FYI

Over the FYI transect, multiscale variability in snow depth was encountered with in situ measurements ranging from 0.0 to 100.9 cm (Figure 1b). At the point scale ($n = 33409$), these measurements compose a lognormal distribution with a mean of 17.8 ± 9.9 cm. The observed distribution and associated length scales of variability are likely to have been heavily influenced by local-scale variations in ice-type and surface topography [*Sturm et al*., 2002]. Variability in ice surface roughness was apparent in RADARSAT-2 imagery collected on 24 March 2014 indicating discontinuous sections of deformed FYI along the in situ transect (Figure 1b). Using a K-Means classification of the RADARSAT-2 imagery and binary reclassification based on a priori knowledge [*Gill and Yackel*, 2012], approximately 38% of the in situ measurements were found to be located within regions of deformed FYI. Snow depths within these areas were generally deeper (20.7 ± 11.4 cm) than those located within the spatially predominate pans of unreformed FYI (16.0 ± 8.3). Increased snow retention was a direct result of the presence of rubble fields, rafted ice, and pressure cracks typically absent within the comparatively homogenous and windswept pans of undeformed FYI.

While regionalized variations in snow depth can be identified in Figure 1b, point-to-point differences in excess of 10 cm appeared to be common over short distances (i.e., < 20 m). This general observation is supported by previous studies of local-scale variability where length scales on the order of tens of meters have been reported independent of ice type [e.g., *Iacozza and Barber,* 1999; *Sturm et al.,* 2002]. Given the bidirectional nature of the FYI transect, there were sufficient in situ pairs to evaluate local-scale variability in both long- and across-track directions. Figure 2a shows variograms constructed from the FYI in situ measurements where a plateau in semivariance was reached at distances subscale to the QL product. Applying an exponential fit, the range was identified at ~12 m after monotonic increases in semivariance in both directions. The short distance to the range shown here is indicative of local-scale heterogeneity and is in agreement with the findings of *Sturm et al.* [2002] who attribute this variability to complex ice roughness and surface process interactions. To maintain a strong assumption of correlation between the field and airborne data sets, QL estimates displaced from the in situ measurements at distances greater than 12 m were removed from further analysis.

Figure 2b shows a comparison of the averaged in situ measurements ($n = 1159$) and colocated QL estimates along the FYI transect ($n = 849$). Following averaging ($n = 1159$), the mean of the in situ measurements remained largely unchanged with a small reduction in standard deviation to 5.9 cm. Over the extent of the FYI transect, the in situ measurements were consistently deeper than the QL estimates with mean values of 17.5 (±5.9) and 12.2 (±4.3) cm, respectively. Overall, the observed mean bias (5.3 cm) appears to fall within the expected uncertainty given by *Kurtz et al.* [2013] but is clearly shifted in distribution (Figure 2b). Possible contributions to the observed bias may include (1) variability in snow density, (2) the finite-range resolution of the snow radar, and (3) misidentification of the air-snow and/or snow-ice interfaces [*Kwok et al*., 2011; *Kurtz et al*., 2013; *Holt et al*., 2015]. While the observed snow density was lower (306 ± 58 kg m^{-3}, $n = 174$) than the assumed OIB value of 320 kg m^{-3}, the disagreement explains errors only on the order of millimeters [*Kwok et al*., 2011]. Given the shallow nature of the snowpack and finite range resolution of the snow radar (~5 cm in free space), it is possible that a distributed set of retrievals fell within a minimum level of detectable snow depth (~8–11 cm from *Kwok et al*. [2011], *Newman et al.* [2014], and *Holt et al*. [2015]). In this regard, only 9% of the averaged in situ depths were less than 11 cm with a majority concentrated near the 15 km mark where exposure to the wind was greatest due to the intersection of Sildre Fijord.

From the QL product alone, it was difficult to attribute instances of interface misidentification to either geophysical or system-based uncertainty. It was, however, possible to identify regions associated with

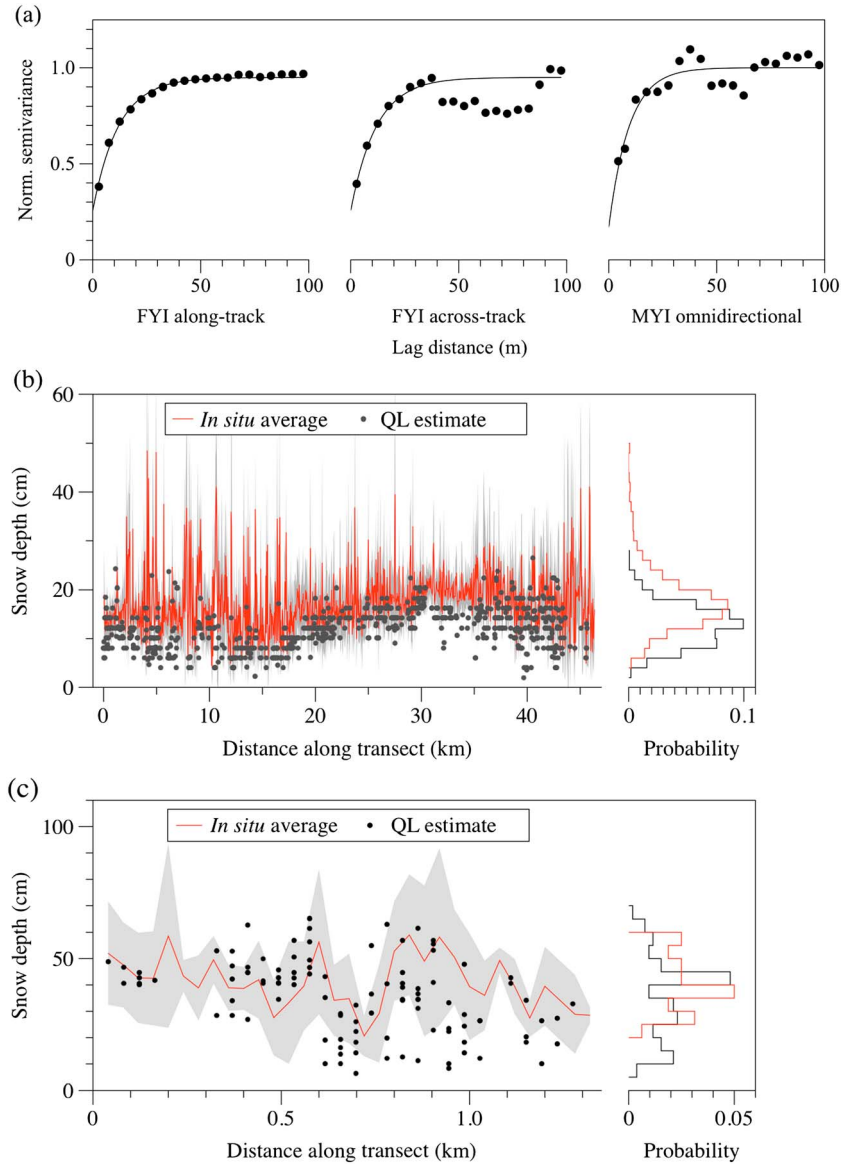

Figure 2. (a) Variograms for the FYI and MYI sites. Snow depths and QL retrievals along the (b) FYI and (c) MYI transects. Red lines show the 40 m in situ mean and standard deviation is shaded in grey. Probability distributions use 2 cm bins for the FYI site and 5 cm for the MYI site.

uncertainty where as part of the OIB retrieval estimates are discarded if there is insufficient signal strength to identify the air-snow interface [*Kurtz et al.,* 2013]. At the FYI site, ~10% of retrievals were discarded by this process with instances apparent across the full range of encountered depth. Assignment of ice type based on the previous RADARSAT-2 classification indicated that discarded retrievals over deformed FYI outnumber those over undeformed FYI by nearly 3:1. In addition to fewer discarded estimates, better agreement with the in situ observations was generally found over the smoother ice regions. Specifically, the observed bias was larger in the deformed ice regions near the origin and terminus of the FYI transect (−6.6 cm) and reduced within the smoother midtransect region (−4.5 cm). Overall, the systematic nature of the observed bias, as well as evidence of roughness based uncertainty, suggests that both system-based and geophysical uncertainties contributed to the observed disagreement at the FYI site.

3.1.2. MYI

Variability in snow depth was considerable at the MYI site (41.5 ± 19.6 cm), consistent with the complex nature of the local surface topography. Drifted snow features transecting the in situ sampling direction

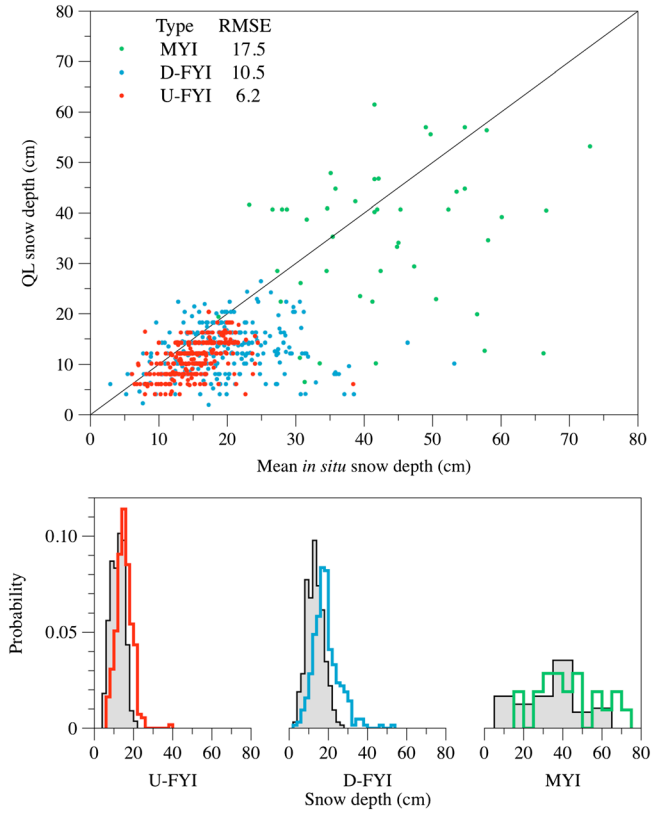

Figure 3. (top) Comparison of measured and retrieved snow depths discretized by undeformed (U-FYI), deformed (D-FYI), and multiyear (MYI) ice types. Root-mean-square error (RMSE) is shown in the legend. (bottom) The probability distributions are shown with 2 cm bins for the FYI sites and 5 cm for the MYI site.

contributed to the extended range of depth from 7.2 to 122.4 cm. Spatially averaged ($n = 33$), the mean depth was comparable to the point scale and again reduced in standard deviation (41.2 ± 10.2 cm). Much like at the FYI site, pairs of in situ measurements were correlated over short distances as indicated by the omnidirectional variogram range of ~10 m (Figure 2a). To maintain a consistent comparison approach, QL estimates displaced at distances greater than the 10 m range were removed from further analysis ($n = 230$).

At the MYI site, the averaged in situ measurements (41.1 ± 10.2) were again deeper than the QL estimates (33.7 ± 14.6), resulting in a negative bias of 5.7 cm (Figure 2c). Although this bias was comparable to the FYI site, an increased number of QL estimates were discarded representing 54% of potential estimates. The discarded retrievals showed increased frequency in proximity to a young pressure ridge near the southern origin of the transect (Figure 1b). Heavily deformed ice near this feature may behave similarly to ridges and rafts noted as problematic by *Farrell et al.* [2012] and others. In such instances, coherent averaging used in the radar processing can reduce signal strength by integrating strong point-to-point variations over short distances making identification of the required snow interfaces difficult or impossible [*Kwok and Maksym*, 2014]. Shape and orientation of drift features may also have played an important role in the observed bias where *Newman et al.* [2014] suggest that stronger returns and lower signal-to-noise are associated with broader snow features relative to the radar footprint. The linear nature and perpendicular orientation of the deep drifts may have made detection difficult and contributed to the observed bias.

3.2. Footprint-Scale Comparison

To further investigate retrieval skill in the QL product, colocated in situ measurements were compared by reconstructing an approximation of the OIB surface projected footprint. At a mean flight elevation of ~472 m, the average across-track footprint was ~10 m in diameter at both sites. Eliminating footprints with less than 10 colocated in situ measurements, 596 were available for evaluation with an average of 22 extracted measurements at the FYI site. At the MYI site, the limited number of in situ measurements left only 48 footprints available for comparison with an average of eight colocated in situ measurements.

Footprint-scale comparison with the extracted in situ measurements is shown in Figure 3. Those over FYI have been further subset into undeformed and deformed components based on the results of the previous RADARSAT-2 classification. As in the previous section, retrievals over undeformed FYI exhibited the best agreement with a root-mean-square error (RMSE) of 6.2 cm and moderate correlation of 0.46 ($p < 0.01$). This finding is in agreement with *Webster et al.* [2014] who reported an RMSE of 5.8 cm over level FYI using the OIB archival product. A number of strong and low-biased outliers appear to have contributed to the moderate correlation over level ice. The observed correlation may also relate to uncertainties unaccounted

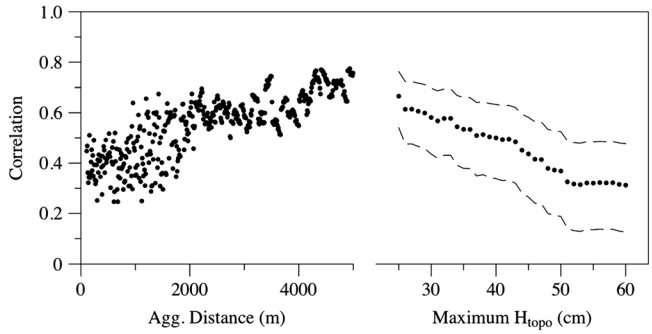

Figure 4. Correlation between the QL retrievals and in situ measurements as a function of (left) aggregation and (right) as a function of maximum h_{topo} between 25 and 55 cm. Dotted lines show the 95% confidence intervals.

for in the retrieval or analysis methods including geolocation errors, variations in flight attitude, heterogeneous snow properties, and inequalities in the point-scale in situ characterization of the two-dimensional snow radar footprint. Retrieval agreement deteriorates over deformed FYI where the RMSE increased to 10.5 cm with a poor correlation coefficient of 0.14 (not statistically significant). Here the QL retrievals appear to be insensitive to increasing snow depth which represents the positive tail of the observed distribution. As expected, retrievals at the MYI site represented the poorest retrieval agreement with an RMSE of 17.5 cm, although with an improved correlation over the deformed FYI ($R = 0.31$).

In practical application, QL estimates of snow depth on sea ice may be used at resolutions other than 40 m in order to evaluate coarser satellite derived products or gridded model output. Figure 4 (left) illustrates the influence of spatial aggregation using a running mean of the QL estimates between 100 m and 5000 m. A clear improvement in the correlation was found with aggregation across distances approaching 5000 m. This result is of particular interest as it suggests that uncertainties unaccounted for at the footprint scale are masked or reduced in influence at scales approaching satellite observation. There was insufficient data to support this type of scaling at the MYI site where the spatial extent was limited.

3.3. Surface Roughness Uncertainty

As previous studies have pointed out, uncertainty associated with ice type and by inference variation in ice surface roughness is common to OIB estimates of snow depth [*Farrell et al.*, 2012; *Newman et al.*, 2014]. We have shown here that QL estimates are more uncertain over regions of deformed ice. As introduced by *Newman et al.* [2014], roughness can be quantified in OIB products using ATM data. The suggested approach uses the difference of the 95th and 5th percentile of 200 ATM ice surface elevations nearest to the OIB snow radar footprint to derive the metric h_{topo}. In complex ice environments, this approach can be used to identify potentially erroneous retrievals where values of h_{topo} exceed the height of the largest expected snow surface features (e.g., drifts, dunes, or sastrugi). In such cases, ice deformation features may be misidentified as snow interfaces in the radar return leading to ambiguous snow depth retrievals.

Values of h_{topo} at the FYI site ranged between 17 and 78 cm with a mean of 27 cm. Diverse surface topography at the MYI site accounted for an elevated mean of 41 cm across a comparable range of 22 to 84 cm. To assess uncertainty associated with increasing surface roughness, correlation between the footprint-scale in situ depth and QL-retrieved snow depth was evaluated using dynamic h_{topo} thresholds. To do so, QL snow depth estimates meeting a maximum h_{topo} threshold were selected for comparison in groups of 100. Random draws were completed 10,000 times in 1 cm increments of the h_{topo} threshold, and correlations were averaged. Testing outside the described range was not possible due to the low number of samples available at the tails of the h_{topo} distribution. Figure 4 (right) shows an inverse relationship between maximum h_{topo} and correlation. For low values of h_{topo}, correlations are comparable to previous studies completed over undeformed FYI (i.e., ~0.6 in *Farrell et al.* [2011]). As h_{topo} increases, it is evident that surface roughness presents a significant geophysical problem for QL snow depth retrievals. It is important to note, however, that from the QL data alone, it is unclear if this is a result of erroneous retrievals or inadequacies in the in situ sampling. Given the shallow snowpack at the FYI site (17.8 cm mean), it is possible that the QL retrieval is sensitive to even small ice deformations requiring careful consideration when used at the footprint scale.

4. Conclusions

The uncertainty of OIB QL estimates of snow depth on sea ice were evaluated using a new data set of comprehensive and extensive coincident in situ measurements. With an RMSE of 6.2 cm, the retrieval over

undeformed FYI approached the uncertainty of the final archived OIB product (5.7 cm). QL retrievals over deformed FYI were characterized by an increased RMSE (10.5 cm) and lacked correlation with the collocated in situ measurements. MYI was the most difficult retrieval environment with an RMSE of 17.5 cm and a substantial number of discarded retrievals (~54%) due to complications related to the highly variable ice surface. Increased strength in the correlation was found by progressively increasing the along-track aggregation length toward 5000 m. Finally, the metric h_{topo} was used to evaluate the influence of surface roughness on retrieval skill. Consistent degradation of correlation between the in situ measurements and QL retrievals was noted with increasing surface roughness.

Overall, this evaluation of the QL estimates of snow depth on sea ice suggests that the product has potential in level ice environments but warrants caution when used in environments of high surface roughness or at scales approaching the 40 m product resolution. Currently unaddressed uncertainties in this study include spatial variations in snow density, stratigraphy, and salinity, which will be evaluated in future work using additional high-density and gridded data sets collected at the FYI and MYI sites. Future study will also need to consider system-based uncertainties to address errors related to the radar signal processing and in situ comparison methods. Lastly, we note that the method used in the QL snow depth retrieval method is largely empirical. New retrieval methods which incorporate the physics of radar returns from snow-covered sea ice surfaces [e.g., *Kurtz et al.,* 2014] are being investigated to improve the quality of the snow depth data set over rough surfaces.

Acknowledgments
OIB data sets used in this letter are available from the NSIDC. QL estimates can be found at https://nsidc.org/data/docs/daac/icebridge/evaluation_products/sea-ice-freeboard-snow-depth-thickness-quicklook-index.html, data sets: OIB_20140325_IDCSI2 and OIB_20140331_IDCSI2. OIB ATM and POS/AV instrument data are found at http://nsidc.org/data/icebridge/instr_data_summary.html, data sets: ILATM1B_20140325*, ILATM1B_20140331*, sbet_20140325, and sbet_20140331. FYI field measurements may be obtained from Environment Canada. MYI field measurements are available at https://earth.esa.int/web/guest/campaigns. RADARSAT-2 imagery used in this letter was made available from the CSA/PSTG and can be acquired for a fee through the National Earth Observation Data Framework web page (https://neodf.nrcan.gc.ca/neodf_cat3/). The FYI field campaign was funded by the Canadian Space Agency through the Government Related Initiatives Program (GRIP). The MYI field campaign was funded by the European Space Agency (ESA) through the CryoSat Validation Experiment (CryoVEx) program. We acknowledge additional support from the Canada Research Chair program. Thank you to the OIB flight and science teams for their efforts to coordinate data collection. Thank you to Bruce Elder and Chris Hiemstra for their contributions to the CryoVEx field campaign.

References

Armitage, T. W. K., and A. L. Ridout (2015), Arctic sea ice freeboard from AltiKa and comparison with CryoSat-2 and Operation IceBridge, *Geophys. Res. Lett.*, *42*, 6724–6731, doi:10.1002/2015GL064823.

Beckers, J. F., C. Haas, B. Elder, C. Hiemstra, R. Tilling, and T. W. K. Armitage (2015), CryoVEx2014—In-situ measurements at MIZ/ONR and NORD (Greenland) ice camps, ESA Ground Team Report, ESA contract 4000110552/14/MP/vb, 46 pp.

Brucker, L., and T. Markus (2013), Arctic-scale assessment of satellite passive microwave-derived snow depth on sea ice using Operation IceBridge airborne data, *J. Geophys. Res. Oceans*, *118*, 2892–2905, doi:10.1002/jgrc.20228.

Comiso, J. C., D. J. Cavalieri, and T. Markus (2003), Sea ice concentration, ice temperature, and snow depth using AMSR-E data, *IEEE Trans. Geosci. Remote Sens.*, *41*(2), 243–252, doi:10.1109/TGRS.2002.808317.

Dominguez, R. (2010), IceBridge POS/AV L1B corrected position and attitude data (2014), NASA DAAC at the Natl. Snow and Ice Data Cent., Boulder, Colo., doi:10.5067/XILTNL9F1HCR. [Updated 2015.]

Farrell, S. L., N. Kurtz, L. N. Connor, B. C. Elder, C. Leuschen, T. Markus, D. C. McAdoo, B. Panzer, J. Richter-Menge, and J. G. Sonntag (2012), A first assessment of IceBridge snow and ice thickness data over Arctic sea ice, *IEEE Trans. Geosci. Remote Sens.*, *50*(6), 2098–2111, doi:10.1109/TGRS.2011.2170843.

Giles, K. A., S. W. Laxon, D. J. Wingham, D. W. Wallis, W. B. Krabill, C. J. Leuschen, D. McAdoo, S. S. Manizade, and R. K. Raney (2007), Combined airborne laser and radar altimeter measurements over the Fram Strait in May 2002, *Remote Sens. Environ.*, *111*(2), 182–194, doi:10.1016/j.rse.2007.02.037.

Gill, J. P. S., and J. J. Yackel (2012), Evaluation of C-band SAR polarimetric parameters for discrimination of first-year sea ice types, *Can. J. Remote Sens.*, *38*(3), 306–323, doi:10.5589/m12-025.

Holt, B., M. P. Johnson, D. Perkovic-Martin, and B. Panzer (2015), Snow depth on Arctic sea ice derived fromradar: In situ comparisons and time series analysis, *J. Geophys. Res. Oceans*, *120*, 4260–4287, doi:10.1002/2015JC010815.

Iacozza, J., and D. G. Barber (1999), An examination of the distribution of snow on sea ice, *Atmos. Ocean*, *37*(1), 21–51, doi:10.1080/07055900.1999.9649620.

Kern, S., K. Khvorostovsky, H. Skourup, E. Rinne, Z. S. Parsakhoo, V. Djepa, P. Wadhams, and S. Sandven (2015), The impact of snow depth, snow density and ice density on sea ice thickness retrieval from satellite radar altimetry: results from the ESA-CCI Sea Ice ECV Project Round Robin Exercise, *Cryosphere*, *9*, 37–53, doi:10.5194/tc-9-37-2015.

Koenig, L., S. Martin, M. Studinger, and J. Sonntag (2010), Polar airborne observations fill gap in satellite data, *Eos Trans. AGU*, *91*(38), 333–334, doi:10.1029/2010EO380002.

Krabill, W. B. (2013), IceBridge ATM L1B Elevation and Return Strength (2014), NASA DAAC at the Natl. Snow and Ice Data Cent., Boulder, Colo., doi:10.5067/19SIM5TXKPGT. [Updated 2015.]

Kurtz, N. T., and S. L. Farrell (2011), Large-scale surveys of snow depth on Arctic sea ice from operation IceBridge, *Geophys. Res. Lett.*, *38*, L20505, doi:10.1029/2011GL049216.

Kurtz, N. T., S. L. Farrell, M. Studinger, N. Galin, J. P. Harbeck, R. Lindsay, V. D. Onana, B. Panzer, and J. G. Sonntag (2013), Sea ice thickness, freeboard, and snow depth products from Operation IceBridge airborne data, *Cryosphere*, *7*, 1035–1056, doi:10.5194/tc-7-1035-2013.

Kurtz, N. T., N. Galin, and M. Studinger (2014), An improved CryoSat-2 sea ice freeboard retrieval algorithm through the use of waveform fitting, *Cryosphere*, *8*, 1217–1237, doi:10.5194/tc-8-1217-2014.

Kwok, R., and C. Haas (2015), Effects of radar sidelobes on snow depth retrievals from Operation IceBridge, *J. Glaciol.*, *61*(227), doi:10.3189/2015JoG14J2292015.

Kwok, R., and T. Maksym (2014), Snow depth of the Weddell and Bellingshausen sea ice covers from IceBridge surveys in 2010 and 2011: An examination, *J. Geophys. Res. Oceans*, *119*, 4141–4167, doi:10.1002/2014JC009943.

Kwok, R., B. Panzer, C. Leuschen, S. Pang, T. Markus, B. Holt, and S. Gogineni (2011), Airborne surveys of snow depth over Arctic sea ice, *J. Geophys. Res.*, *116*, C11018, doi:10.1029/2011JC007371.

Lindsay, R., C. Haas, S. Hendricks, P. Hunkeler, N. Kurtz, J. Paden, B. Panzer, J. Sonntag, J. Yungel, and J. Zhang (2012), Seasonal forecasts of Arctic sea ice initialized with observations of ice thickness, *Geophys. Res. Lett.*, *39*, L21502, doi:10.1029/2012GL053576.

Maass, N., L. Kaleschke, X. Tian-Kunze, and R. T. Tonboe (2015), Snow thickness retrieval from L-band brightness temperatures: A model comparison, *Ann. Glaciol.*, *56*(69), 9–17, doi:10.3189/2015AoG69A886.

Newman, T., S. L. Farrell, J. Richter-Menge, L. N. Connor, N. T. Kurtz, B. C. Elder, and D. McAdoo (2014), Assessment of radar-derived snow depth over Arctic sea ice, *J. Geophys. Res. Oceans*, *119*, 8578–8602, doi:10.1002/2014JC010284.

Panzer, B., D. Gomez-Garcia, C. Leuschen, J. Paden, F. Rodriguez-Morales, A. Patel, T. Markus, B. Holt, and P. Gogineni (2013), An ultrawide-band, microwave radar for measuring snow thickness on sea ice and mapping near-surface internal layers in polar firn, *J. Glaciol.*, *59*(214), 244–254, doi:10.3189/2013JoG12J128.

Perovich, D. K., T. C. Grenfell, J. A. Richter-Menge, B. Light, W. B. Tucker, III, and H. Eicken (2003), Thin and thinner: Sea ice mass balance measurements during SHEBA, *J. Geophys. Res.*, *108*(C3), 8050, doi:10.1029/2001JC001079.

Perovich, D. K., S. V. Nghiem, T. Markus, and A. Schweiger (2007), Seasonal evolution and interannual variability of the local solar energy absorbed by the Arctic sea ice–ocean system, *J. Geophys. Res.*, *112*, C03005, doi:10.1029/2006JC003558.

Ricker, R., S. Hendricks, D. K. Perovich, V. Helm, and R. Gerdes (2015), Impact of snow accumulation on CryoSat-2 range retrievals over Arctic sea ice: An observational approach with buoy data, *Geophys. Res. Lett.*, *42*, 4447–4455, doi:10.1002/2015GL064081.

Sturm, M., J. Holmgren, and D. K. Perovich (2002), Winter snow cover on the sea ice of Arctic Ocean at the Surface Heat Budget of the Arctic Ocean (SHEBA): Temporal evolution and spatial variability, *J. Geophys. Res.*, *107*(C10), SHE 23-1–SHE 23-17, doi:10.1029/2000JC000400.

Sturm, M., J. A. Maslanik, D. K. Perovich, J. C. Stroeve, J. Richter Menge, T. Markus, J. Holmgren, J. F. Heinrichs, and K. Tape (2006), Snow depth and ice thickness measurements from the Beaufort and Chukchi Seas collected during the AMSR-Ice03 campaign, *IEEE Trans. Geosci. Remote Sens.*, *44*(11), 3009–3020, doi:10.1109/TGRS.2006.878236.

Webster, M. A., I. G. Rigor, S. V. Nghiem, N. T. Kurtz, S. L. Farrell, D. K. Perovich, and M. Sturm (2014), Interdecadal changes in snow depth on Arctic sea ice, *J. Geophys. Res. Oceans*, *119*, 5395–5406, doi:10.1002/2014JC009985.